

Light emitting charge injection transistor with *p*-type collector

Marco Mastrapasqua, Federico Capasso, Serge Luryi, Albert L. Hutchinson,
Deborah L. Sivco, and Alfred Y. Cho
AT&T Bell Laboratories, Murray Hill, New Jersey 07974

(Received 27 December 1991; accepted for publication 20 March 1992)

We report the first realization of a charge injection transistor with a complementary collector. The device is implemented using InGaAs/InAlAs/InGaAs heterostructure material grown by molecular beam epitaxy. Real space transfer of hot electrons into the *p*-type collector leads to a luminescence signal arising from the recombination of the injected electrons with holes in the collector active region. The observed on/off ratio in the emitted light power is more than 10^4 and obeys an exclusive OR function of input voltages. The estimated internal quantum efficiency is as high as 90%.

Charge-injection transistors (CHINT), based on real space transfer¹ (RST) of hot electrons between two independently contacted conducting layers, have been widely studied both theoretically and experimentally.² In all experimental studies the type of conductivity was the same in both layers connected by the RST (the emitter channel and the collector). Recently, one of us discussed³ the RST of *minority carriers* into a collector layer of complementary conductivity type. This allows the implementation of light emitting devices and lasers endowed with logic functions, such as exclusive OR. New logic opportunities result from the fact that the RST current is independent of the polarity of the electron-heating field.⁴

In this letter, we report the first realization of a CHINT with an *n*-type emitter channel and a *p*-type collector. The lattice-matched InGaAs/InAlAs/InGaAs heterostructure was grown by molecular beam epitaxy (MBE) on a semi-insulating InP substrate. Figure 1(a) shows a cross section of the device obtained after several selective etching steps and a Si₃N₄ deposition. The *n*⁺ cap layer is removed in the trench area. The channel length, defined by the trench, is 3 μm and the width 50 μm. After the etching, the exposed portion of the channel is entirely depleted by the surface potential, so that the channel conduction relies on a positive collector voltage.

Electron heating is generated by a drain-to-source bias V_{DS} . The real-space transfer manifests itself in the increasing collector current I_C and the recombination radiation from the *p*-type collector. It is accompanied by a negative differential resistance in the drain current I_D . The purpose of the wide-gap *p*⁺ InAlAs layer in the collector is to confine spatially the electrons injected over the barrier by RST and, at the same time to provide a low-resistance path for the collector current.

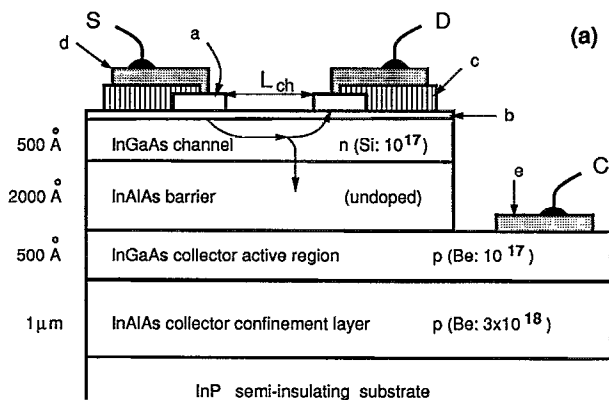
The device was first characterized electrically. Figure 1(b) shows the collector leakage current, with both source and drain grounded, as a function of the collector bias V_C for different temperatures. The collector-channel diode represents a forward-biased *p-n* junction, with a barrier in between. Because of the different discontinuities in the valence and the conduction bands ($\Delta E_V \approx 0.2$ eV and $\Delta E_C \approx 0.5$ eV) the leakage current is mainly due to the transport of holes from the collector to the channel. At high temperatures, $200 < T < 300$ K, and relatively low bias, the

current obeys the thermionic model $I_C = I_C^{(0)} e^{qV_C/nkT}$, with an ideality factor $n = 1.4$ and a saturation current $I_C^{(0)} = SA^*T^2 e^{-\Phi/kT}$, where $S \approx 10^{-5}$ cm² is the total emitter area including the source and drain contacts, Φ is the barrier height at zero bias (separation between the hole Fermi level in the collector and the valence band edge in the barrier at the channel interface), and A^* the effective Richardson constant. The inset to Fig. 1(a) shows an Arrhenius plot of $I_C^{(0)}/T^2$ versus T^{-1} in the high-temperature range. The slope of this plot gives $\Phi = 0.90$ eV in agreement with a calculated value $\Phi \approx 0.91$ eV, based on the energy gap $E_G = 0.75$ eV of InGaAs, the valence-band discontinuity $\Delta E_V \approx 0.2$ eV and given doping levels. Extrapolating $\log [I_C^{(0)}/T^2]$ to $T^{-1} \rightarrow 0$, we find $A^* \approx 72$ A cm⁻² K⁻² in reasonable agreement with the theoretical value for heavy holes.

At higher V_C (exceeding the flat-band condition) the top of the barrier for holes is at the collector interface. This is the operating regime of a complementary CHINT. The barrier height further decreases with V_C because of the accumulation of holes (increasing the Fermi level) and also, effectively, due to thermally assisted tunneling. At low temperatures, $T < 150$ K, thermally assisted tunneling of holes is the dominant leakage mechanism. As is evident from Fig. 1(b), in the operating regime the slope of $\log I_C(V_C)$ is relatively gentle.

Figures 2(a) and 2(b) describe the current-voltage characteristics at $T = 235$ and 100 K. At a fixed V_C and increasing the heating voltage V_{DS} , the channel current first increases like in a field-effect transistor. When V_{DS} is high enough to establish a significant RST, the drain current shows a negative differential resistance (NDR). Simultaneously, the collector current rapidly increases from its leakage value. In the high- T plot, Fig. 2(a), the collector current is seen to decrease prior to the onset of NDR. This is due to the diminishing leakage current (roughly by a factor of 2), with decreasing collector-to-drain bias. This effect is shown by the dotted line, computed from the leakage curve in Fig. 1(b). The same behavior occurs at low temperatures but on the scale of Fig. 2(b) the leakage is not resolved.

The existence of a maximum in I_C and the decrease of I_C at higher V_{DS} is related to the increase in the potential of the "hot spot" (i.e., the high-field region in the channel



- a: 200 Å InGaAs, n (Sn: 10^{20})
 b: 25 Å InAlAs, n (Sn: 10^{19})
 c: 2500 Å Si_3N_4
 d: 300 Å Ti / 1800 Å Au
 e: 800 Å AuBe / 2000 Å Au

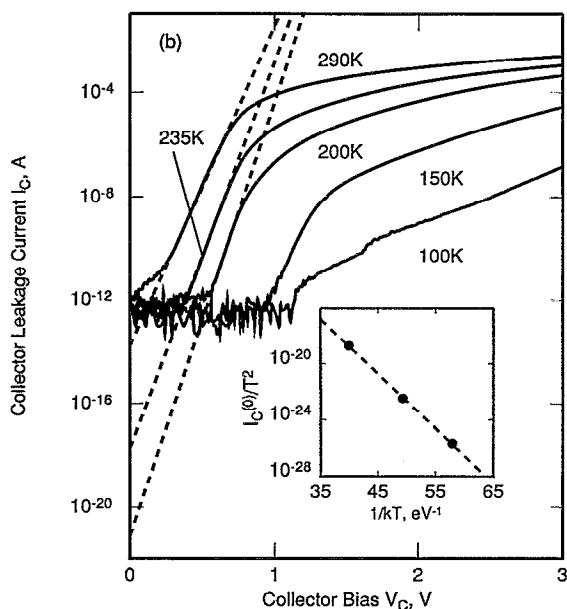


FIG. 1. (a) Cross section of the sample structure. The real-space transfer current is indicated by the downward arrow. (b) Collector current-voltage characteristics (source and drain grounded) at different temperatures. Dashed lines indicate the linear extrapolation of I_C to zero forward bias. The intercepts of the dashed lines with the ordinate axis correspond to $I_C^{(0)}$. Inset shows an Arrhenius plot of $I_C^{(0)}/T^2$.

where most of the RST occurs) relative to the collector. Reversal of the field in the barrier suppresses the RST at the hot spot and the device effectively goes out of the operating range discussed in connection with Fig. 1(b).

The luminescence arising from the recombination of injected electrons in the p -type collector was detected from the back of the polished substrate using a liquid nitrogen-cooled Ge detector and a 0.75 nm spectrometer. We observed a spectrum peaked at 1.59 and 1.56 μm at 235 and 100 K, respectively. To measure the total emitted power, we used a broad-area Ge photodiode and suitable focusing optics. Figure 3 shows the bias dependence of both the drain current I_D and the measured light power P_m . Due to the symmetry property^{3,4} of the CHINT, the output optical power depends only on the magnitude of the heating bias

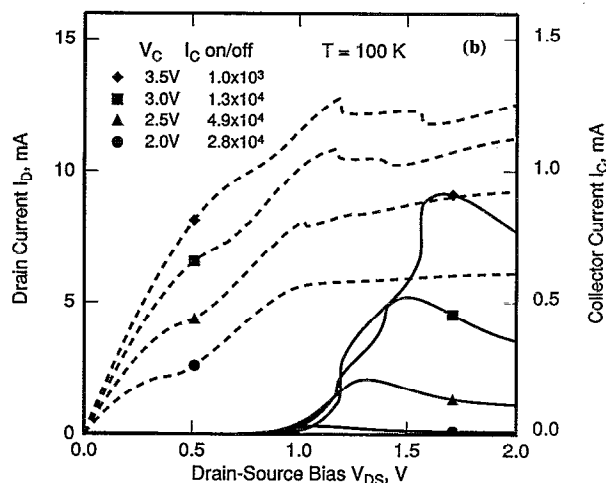
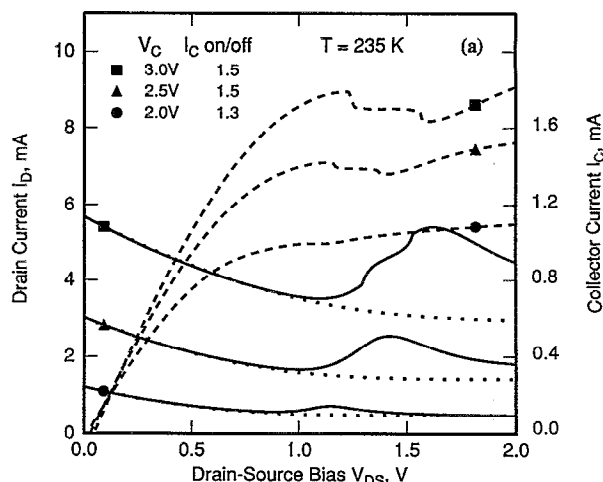


FIG. 2. Current-voltage characteristics at $T=235$ K. (a) and $T=100$ K. (b). Drain current I_D is shown by the dashed line and collector current I_C by the solid line. The dotted lines show the expected leakage behavior of I_C in the absence of RST, calculated from Fig. 1(b). The collector current on/off ratio is calculated by dividing the maximum value of I_C by its minimum value before the onset of real-space transfer.

V_{DS} —and not on its polarity. Thus, the device exhibits an exclusive OR dependence of the emitted light power on the input voltages regarded as logic signals, $P_m = \text{XOR}(V_S, V_D)$.

The fact that the optical on/off ratio (Fig. 3) far exceeds the on/off ratio in the collector current (Fig. 2) confirms that the collector leakage is mostly due to the injection of holes into the channel. These holes are likely to reach the source contact or the surface before they recombine radiatively with electrons. In contrast, electrons injected into the collector are confined in the active region. The fact that the leakage and the RST are caused by different types of carriers implies an important design consideration: to maximize the optical on/off ratio it is essential to suppress the leakage of electrons into the active region; the oppositely directed flux of holes can be tolerated.

At higher T , the small electron component of the leakage current increases and the on/off ratio disparity between the light-power output and the collector current is less pronounced. At room temperature and $V_C=3.0$ V the

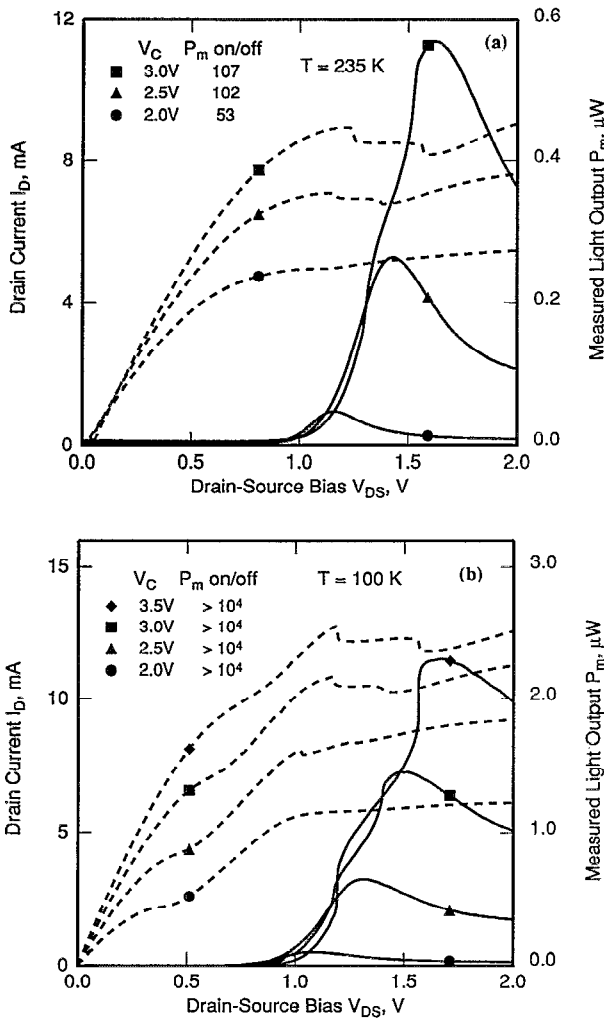


FIG. 3. The total measured light power P_m (solid line) versus the drain-source bias V_{DS} at $T=235$ K (a) and $T=100$ K (b). Dashed lines indicate the drain current I_D from Fig. 2. The light power on/off ratio is calculated by dividing the maximum value of P_m by its minimum value before the onset of real-space transfer.

on/off ratio is 9 in P_m and 1.1 in I_C . At low temperatures, Fig. 3(b), the light signal related to the leakage is below the noise level and the on/off ratio in P_m is above 10^4 .

From the increment of the light power in going from the off to the on state, it is possible to estimate the internal photon generation rate G_{ph} due to the RST:

$$G_{ph} = \frac{P_m}{h\nu\eta_c t_o},$$

where $\eta_c \approx 0.48\%$ is the collection efficiency which takes into account both the total internal reflection and the collection solid angle, $t_o \approx 88\%$ is the combined transmission of the optical components (lens and windows) between the detector and the device, and $h\nu$ is the photon energy at the peak of the luminescence spectrum. Dividing G_{ph} by the RST flux, which is the RST current measured in units of electronic charge, we obtain the internal quantum efficiency η_q plotted in Fig. 4. The RST current is defined as I_C minus the leakage current, computed from Fig. 1(b).

We have found that at a given T and V_C the efficiency is not modulated by varying V_{DS} , which means that η_q is

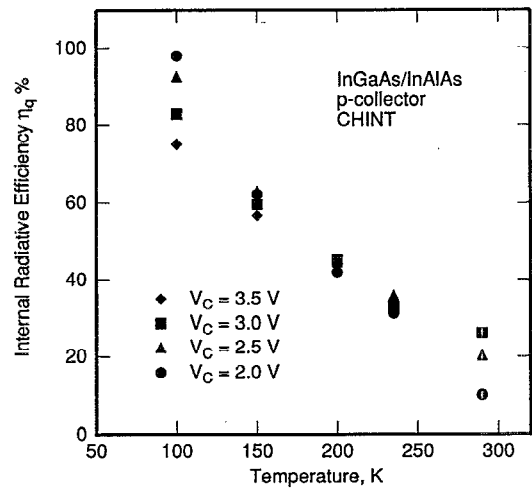


FIG. 4. Dependence of the internal quantum efficiency η_q on the lattice temperature for different collector biases.

independent of the injection current. On the other hand, as seen from Fig. 4, the radiative efficiency decreases with increasing temperature. At low $T \lesssim 150$ K, the efficiency is also seen to decrease with increasing collector bias. This effect is probably related to the injection of hot electrons into the wide-gap collector confinement layer where they recombine nonradiatively.⁵ No significant variation of η_q with V_C is observed at higher temperatures, presumably because of the shorter hot-electron mean-free path (the apparent dependence at $T \gtrsim 200$ K in Fig. 4 is not meaningful since the low- V_C points are within the uncertainty introduced by the subtraction of the leakage component).

In conclusion, we have reported the first CHINT with a complementary p -type collector. In accordance with the theoretical prediction³ the device generates an optical signal that is an exclusive OR function of the voltage inputs applied to the source and drain electrodes. The device exhibits an extremely high light-power on/off ratio, which we explain by analyzing the leakage current and showing that, in contrast to the RST current, it is mainly nonradiative.

We thank E. A. Laskowski for help in selective chemical etching and D. A. Humphrey for Si_3N_4 deposition. M. Mastrapasqua acknowledges the financial support (E. De Castro fellowship) of Associazione Elettrotecnica ed Elettronica Italiana.

¹Z. S. Gribnikov, Sov. Phys. Semicond. **6**, 1204 (1973); K. Hess, H. Morkoç, H. Shichijo, and B. G. Streetman, Appl. Phys. Lett. **35**, 469 (1979).

²Recent references on real-space transfer devices can be found in S. Luryi, Superlatt. Microstruct. **8**, 395 (1990).

³S. Luryi, Appl. Phys. Lett. **58**, 1727 (1991).

⁴S. Luryi, P. Mensz, M. Pinto, P. A. Garbinski, A. Y. Cho, and D. L. Sivco, Appl. Phys. Lett. **57**, 1787 (1990).

⁵Even if there were a radiative component from the confinement layer, it would not be detected experimentally, since all of the InAlAs light output would be re-absorbed in the InP substrate. Moreover, as a matter of principle, one would not expect a significant radiation from the wide-gap layer, since electrons there are no longer confined and their radiative lifetime is longer than travel time to the contact.